







Cite this: *Chem. Commun.*, 2017, 53, 8211

Received 25th May 2017,  
Accepted 23rd June 2017

DOI: 10.1039/c7cc04050d

rsc.li/chemcomm

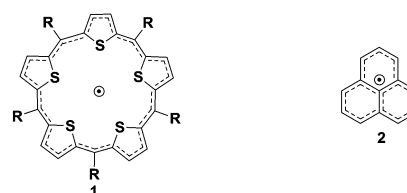
## A naphthalene-fused dimer of an anti-aromatic expanded isophlorin†

Baddigam Kiran Reddy, <sup>‡a</sup> Jeff Rawson, <sup>‡bc</sup> Santosh C. Gaddekar, <sup>a</sup>  
Paul Kögerler <sup>\*bc</sup> and Venkataramanarao G. Anand <sup>\*a</sup>

**We report the first synthesis of a covalent expanded isophlorin dimer from two 24- $\pi$  doubly S-confused sapphyrin-like pentathiaisophlorins. It exhibits marginal peripheral aromaticity rather than strong global diatropicity or paratropicity and weak intermacrocycle electronic communication. Quantum chemical methods discern that cross-conjugation is responsible for these unusual electronic features.**

Aromatic macrocycles such as porphyrin and corrole have attracted significant attention for their unique electronic properties.<sup>1</sup> The oxidative coupling of these individual macrocyclic units, through their *meso* and  $\beta$  carbons, is a frequently employed synthetic strategy to blend them into short oligomers.<sup>2</sup> Multiple intermolecular connectivities enhance the electronic coupling between these adjacent  $\pi$  sub-units leading to exceptional properties such as globally delocalized<sup>2b</sup> and electronically excited states,<sup>3</sup> hole/electron-polaron states,<sup>4</sup> low energy two-photon absorptions<sup>5</sup> and low resistances when sandwiched between metal layers.<sup>6</sup> Compared to the versatile chemistry of aromatic building blocks, inadequate synthetic protocols for structurally similar anti-aromatic macrocycles have hindered the fusion of individual  $4n\pi$  molecules into  $\pi$ -conjugated materials.<sup>7</sup> Even though stable anti-aromatic isophlorinoids hold promise to explore the electronic properties of unheralded fused  $4n\pi$  systems, the enigmatic incompatibility of a *meso*-free isophlorin to oxidative coupling has precluded the direct synthesis of a *meso*-*meso* linked isophlorin dimer.<sup>8</sup> Herein, we report the synthesis of the first fused dimer of an anti-aromatic expanded isophlorin along with its structural and electronic properties.

A recent report established reversible two-electron oxidation of a stable anti-aromatic isophlorin.<sup>9</sup> Prior to this report, a



**Scheme 1** Pentathiophene 25 $\pi$  expanded isophlorin (**1**) and spin delocalization in the phenalenyl radical (**2**).

stable expanded isophlorin, **1**, with 25 $\pi$  electrons was identified as a neutral and stable radical under ambient conditions.<sup>10</sup> It undergoes a facile one-electron oxidation and reduction to generate 24 $\pi$  and 26 $\pi$  diamagnetic species, respectively. Similar, but smaller, organic  $\pi$  radicals exhibit dimerization either through covalent or non-covalent interactions (Scheme 1).

NMR spectroscopic studies of a phenalenyl radical, **2**, confirmed a non-covalent diamagnetic  $\pi$ -dimer at low temperatures.<sup>11</sup> Its sigma dimer also exhibits diamagnetism when fused directly in the absence of any spacer. However, the covalent dimer can exist both as a diamagnetic and paramagnetic species depending on the nature of the link between the two phenalenyl units.<sup>12</sup> Dimerizing **1** through one of its *meso* carbons offers the possibility of a biradical or a closed-shell double bond bridge between the individual macrocyclic units. Further amalgamation through the  $\beta$  positions should yield a completely fused expanded isophlorin dimer. Our recent report on the synthesis of a *meso*-*meso* linked 20 $\pi$  isophlorin dimer established that a bridging double bond results in the formation of unstable biradical species.<sup>8</sup> Such structure-dependent spin states for dimers of expanded porphyrinoids or isophlorinoids have not been explored to date. Anticipating the stabilization of a triple-link between the two 25 $\pi$  pentathiophene radicals, **1**, we designed the synthesis of **3** with appropriate precursors from thiophene units (Scheme 2).

The synthesis involved the condensation of dicarbinol, **4**, with tetrathienylethene, **5**,<sup>13</sup> under acidic conditions followed by oxidation to obtain the desired expanded isophlorin dimer. A pink band was isolated from the reaction mixture through

<sup>a</sup> Department of Chemistry, Indian Institute of Science Education and Research (IISER), Pune, 411008, Maharashtra, India. E-mail: vg.anand@iiserpune.ac.in

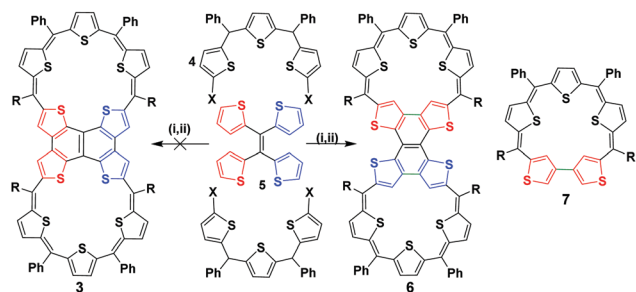
<sup>b</sup> PGI-6, Forschungszentrum Jülich, 52428 Jülich, Germany

<sup>c</sup> Institute of Inorganic Chemistry, RWTH Aachen University, 52074 Aachen, Germany. E-mail: paul.koegerler@ac.rwth-aachen.de

† Electronic supplementary information (ESI) available. CCDC 1476102 for X-ray crystal structure of **6**. For ESI and crystallographic data in CIF or other electronic format see DOI: 10.1039/c7cc04050d

‡ These authors contributed equally.





**Scheme 2** Acid-catalysed synthesis of expanded isophlorin **6**. Reaction conditions: (i)  $\text{BF}_3 \cdot \text{OEt}_2$  (1 eq.), dry DCM (100 ml), rt,  $\text{N}_2$ , 2 h (ii)  $\text{FeCl}_3$  (10 eq.), 2 h.  $\text{X} = -\text{CH}(\text{OH})\text{R}$ ,  $\text{R} = \text{C}_6\text{F}_5$ . **7** represents the structural isomer of a doubly confused pentathiasapphyrin.

silica gel column chromatography with dichloromethane and hexane as the eluent. After evaporation of the solvent under vacuum, the obtained green solid (in 10% yield) displayed an  $m/z$  value of 1911.7206 corresponding to the mass of a triply linked dimer **3** from MALDI-TOF-TOF mass analysis. This confirmed both cyclization and the expected oxidative dehydrogenation of the thiophene beta carbons in the presence of  $\text{FeCl}_3$ . Owing to the limited solubility of the isolated dimer **6**, attempts to crystallize it in various solvent systems went futile until we were successful by adding a few drops of TFA in a solution of chloroform. The molecular structure as determined from single crystal X-ray diffraction analysis revealed a novel and an unusual structural isomer of the expected dimer. This revealed the unexpected condensation of the vicinal thiophene units, instead of the geminal thiophenes, with two units of diol to form the macrocyclic dimer (Fig. 1).

A rare  $\beta$ - $\beta$  oxidative dehydrogenation between the adjacent two ring-inverted thiophene rings yields a sapphyrin-like framework to complete the macrocyclic framework. This unexpected fusion resembles a typical [3+2] condensation employed in the synthesis of ring-inverted sapphyrin.<sup>14</sup>

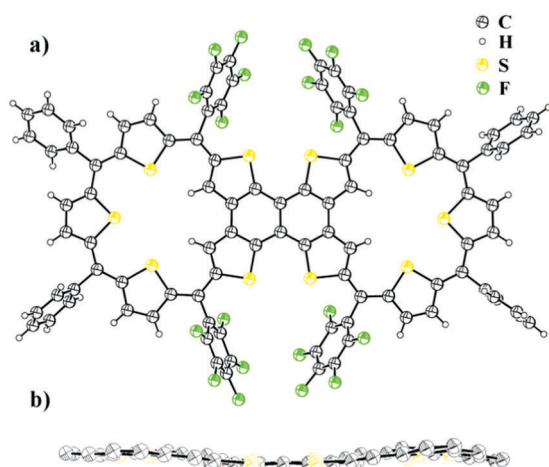


**Fig. 1** (a) Molecular structure of **6** determined from single crystal X-ray diffraction. (b) Side view of compound **6** (*meso*-substituents omitted for clarity).

Surprisingly, the desired dimer, **3**, of a  $25\pi$  radical was not identified in this reaction. In spite of a large structure, with ten thiophene units, the system sustains a relatively flat topology. Compound **6** displayed a near planar structure and the crystal packing shows weak  $\pi$ - $\pi$  interaction with an inter-planar distance of 3.79 Å between adjacent layers (see ESI†). The *meso* phenyl rings have a near orthogonal orientation with respect to the mean plane of the dimer. The ethylene moiety can be a part of aromatic conjugation with only one of the two macrocyclic units. Therefore, it can be considered to be a merger of an aromatic ( $26\pi$  electrons) and an anti-aromatic unit ( $24\pi$  electrons). Yet, the total number of  $50\pi$  electrons corresponds to Hückel's  $(4n + 2)$   $\pi$ -electrons and hence expected to display a diatropic ring current effect. The photocyclization of tetrathienylethene **5** with 366 nm light in the presence of iodine has been shown to give tetrathienonaphthalene,<sup>13</sup> which constitutes a substructure within the framework of **6**, which has limited solubility in common organic solvents, but is modestly soluble in halobenzenes. Similar to this sub-unit, the dimer **6** has poor solubility in common organic solvents. Proton NMR spectroscopy of **6** in chlorobenzene- $d_5$  at 400 K gives chemical shifts of the thiophene  $\beta$ -protons that evidence its weak macrocyclic ring current. In particular, the protons of inverted rings resonate at  $\delta$  5.78 ppm, upfield from 8.1 ppm (in bromobenzene- $d_5$  at 403 K) for the comparable positions on tetrathienonaphthalene. The protons on the two central thiophene rings of the trithiophene sub-unit resonate as a singlet at  $\delta$  7.354 ppm, downfield from 7.09 ppm at the 3-position of thiophene. The remaining two sets of thiophene  $\beta$ -protons evince two doublets centered at  $\delta$  7.436 ppm and 7.289 ppm. The magnitudes of the proton chemical shifts induced by the macrocyclic ring current are substantially smaller than those observed for strongly aromatic  $30\pi$  thiaporphyrinoids.<sup>7</sup>

Analysis of the DFT-calculated magnetic properties of **6** using nucleus-independent chemical shifts at a distance of 1 Å from the macrocycle plane (NICS(1))<sup>15</sup> buttresses the proton NMR evidence of marginal aromatic ring currents in this system (Fig. 2B). While strong local magnetic shieldings are determined for points centered over the internal naphthalene ( $-20.35$  ppm) and central thiophenes ( $-10.47$  ppm), a value of 0.20 ppm is calculated above the centroid of each pentathiophene macrocycle. This contrasts the case of a  $30\pi$  aromatic hexaphyrin, for which a strong shielding NICS(1) value is calculated at the macrocycle center ( $-14.85$  ppm; see ESI†).

The electronic absorption spectrum of **6**, collected in chlorobenzene solution, consists of a low energy ground to first singlet excited state ( $S_0 \rightarrow S_1$ ) transition spanning  $\sim 650$ – $850$  nm with the maximum extinction coefficient  $\epsilon \approx 10^4$ , a tenfold more intense  $S_0 \rightarrow S_2$  peak centred at 567 nm, and a continuous manifold of  $\epsilon \approx 30\,000$  absorption from 350 to 500 nm (Fig. 3). For aromatic porphyrinoids, the  $S_0 \rightarrow S_1$  transition typically gives rise to a series of  $\epsilon = 10^4$  visible-range peaks (Q-band), and a single  $\epsilon > 10^5$  peak at the edge of the UV region (B-band), which may be compared with the  $S_0 \rightarrow S_1$  and  $S_0 \rightarrow S_2$  bands of **6** respectively.<sup>16</sup> However, the strong vibronic splitting of the  $S_0 \rightarrow S_2$  band of **6** is very different from a typical porphyrin Soret transition, which evinces minimal vibronic satellites in spite of its great intensity.<sup>17</sup>



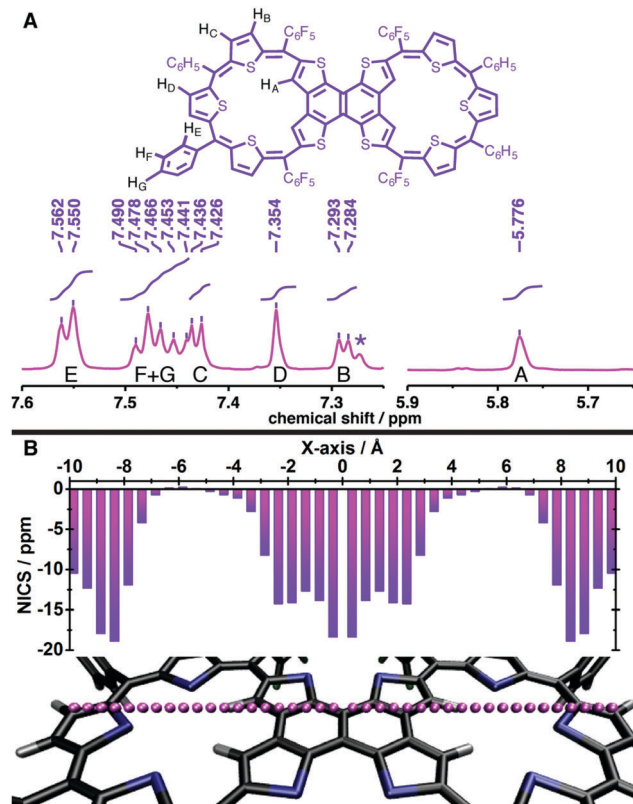


Fig. 2 (A) Selected regions and peak assignments from the  $^1\text{H}$  NMR spectrum of **6** determined at 400 K in chlorobenzene- $d_5$  solvent. The star marks a sideband from a solvent peak. (B) Values of NICS(1) calculated at points along the long molecular axis.

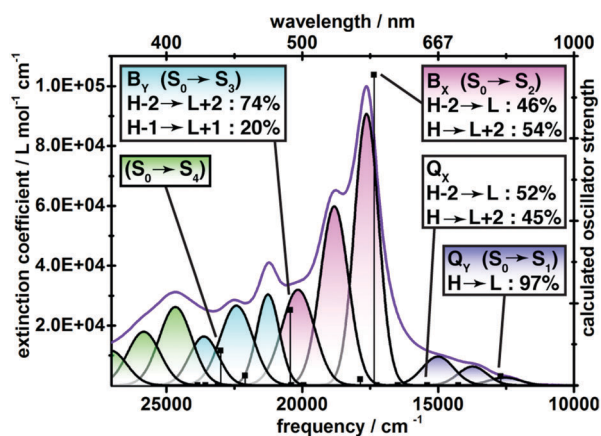


Fig. 3 Electronic absorption spectrum of **6** measured in chlorobenzene solvent and its decomposition into Gaussian sub-bands. Boxes present assignments of major transitions based upon TDDFT calculations, with phenomenological labels in parentheses, and the principle electronic configurations of each transition as determined by population analysis.

The electronic spectrum of **6** is suggestive of a polycyclic benzenoid hydrocarbon rather than a globally aromatic porphyrinoid. A combination of TDDFT calculations and spectral deconvolution into Gaussian peaks identifies four principle electronic transitions within the 350–850 nm wavelength range,

each of which is split into three discernible vibronic sub-bands that are spaced by  $\sim 1200\text{ cm}^{-1}$ . Notably, the long-axis polarized  $\text{Q}_\text{x}$  transition is calculated to be nearly forbidden, and the  $\text{S}_0 \rightarrow \text{S}_1$  manifold is attributed to the  $\text{Q}_\text{y}$  transition. The Y-polarized transitions are essentially a single configuration in nature ( $\text{Q}_\text{y}$ ,  $\text{H} \rightarrow \text{L}$ : 97%;  $\text{B}_\text{y}$ ,  $\text{H}-2 \rightarrow \text{L}+2$ : 74%), while the X-polarized transitions evince strong configuration interaction ( $\text{B}_\text{x}$ ,  $\text{H}-2 \rightarrow \text{L}$ : 46%,  $\text{H} \rightarrow \text{L}+2$ : 54%;  $\text{Q}_\text{x}$ ,  $\text{H}-2 \rightarrow \text{L}$ : 52%,  $\text{H} \rightarrow \text{L}+2$ : 45%). The Q-bands of a  $\text{D}_{4h}$  metalloporphyrin are nearly forbidden,<sup>17</sup> but for porphyrins with extended  $\pi$ -electron systems<sup>18</sup> and many conjugated porphyrin oligomers,<sup>4</sup> symmetry breaking disrupts the configuration interaction to red shift and intensify the long axis-polarized Q-derived states. For **6**, the unobservable  $\text{Q}_\text{x}$  band and its strong configuration interaction-pairing with  $\text{B}_\text{x}$  suggest that the molecule **6** is comprised of two macrocycles that function as separate entities.

The modest electronic coupling down the long axis of the molecule **6** is better understood by constructing a correlation diagram in which the bis-macrocycle is modeled as two S-confused thiasapphyrinoids **7** united by an ethylene bridge (Fig. 4). Note that the ethylene  $\text{b}_{3g}$  and  $\text{b}_{1u}$  wavefunctions are forbidden by symmetry

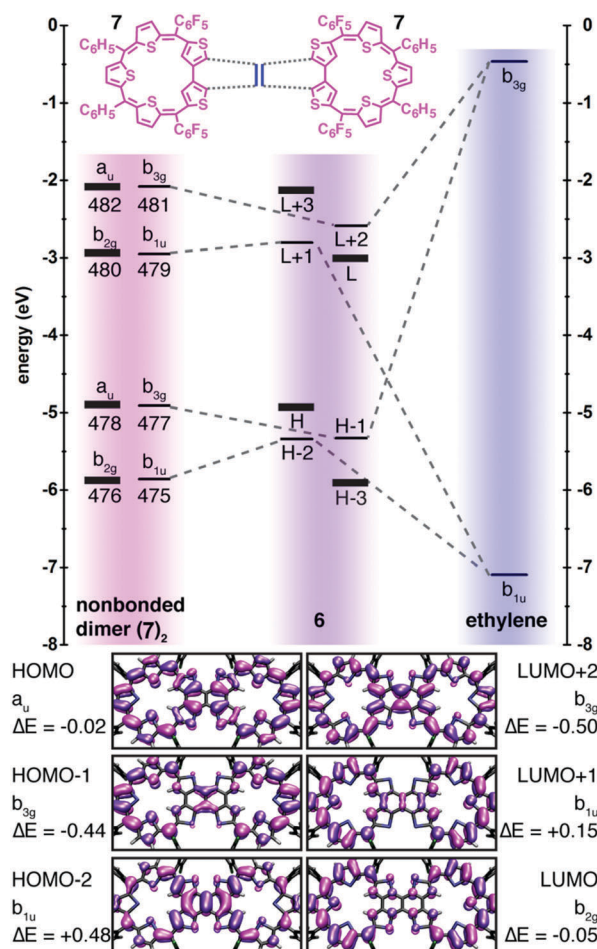


Fig. 4 Top: Correlation diagram that deconstructs **6** into thiasapphyrinoid and ethylene fragments. Bottom: Frontier orbital wave functions of **6** plotted as 0.02 isodensity surfaces, with energy differences between them and their progenitors in the non-bonded thiasapphyrinoid dimer.





from constructive overlap with the thiasapphyrinoid  $a_u$  and  $b_{2g}$  wavefunctions which constitute the HOMO and LUMO of **6**, respectively, and also with the progenitors of H-3 and L+3 of **6**. These orbitals evince nodal planes that bisect the bridge carbons, and their energies are scarcely perturbed from those of their antecedents in the non-bonded dimer. A comparison of the TDDFT-calculated electronic transitions for **7** and **6** further shows that the spectral features evinced by **6** may be ascribed to the through-space excitonic coupling between the two thiasapphyrinoid building blocks in the weak coupling limit (see the ESI† for more details).<sup>19</sup>

The marginal global aromaticity of the macrocycles of **6** and the weak communication between them are consequences of cross-conjugation, where two unsaturated groups are conjugated to a third, but not to each other.<sup>17</sup> The linkage of the putative thiasapphyrinoids **7** by the ethylene bridge is one such instance of cross-conjugation, as this bridge forbids any reasonable resonance structures that push electrons from one ring to the other. The structure of **7** itself contains two exocyclic double bonds at the point where thiophene rings are joined by their  $\beta$ -positions, constituting a doubly cross-conjugated linkage which limits its anti-aromatic character despite the  $24\pi$ -electron count of its circuit. A similarly structured doubly N-confused  $22\pi$  sapphyrin was indeed found to evince a negligible peripheral aromatic ring current.<sup>14</sup> Our experimental and computational evidence supports the significance of this qualitative Lewis structure analysis, yet more desirable would be a quantitative method derived from molecular orbital calculations.

In summary, we have synthesized a novel dimer of an anti-aromatic expanded isophlorin. The synthesis for the first time reveals the oxidative coupling of inverted heterocyclic rings, in contrast to non-inverted heterocyclic rings in aromatic porphyrinoids. The impact of cross-conjugation effects upon molecular conductance resonances<sup>20</sup> and electron transfer rates<sup>21</sup> has been recognized recently, and this structural motif has been prominently explored in annulene chemistry.<sup>22</sup> The decisive influence of cross-conjugation upon macrocycle aromaticity and intermolecular electronic communication outlined here provides another dramatic example of nonlinear conjugation.

Parts of this work were supported through EU ERC grant no. 308051 – MOLSPINTRON. BKR thanks UGC, New Delhi, India, for the research fellowship. VGA thanks DST, New Delhi, India, for the Swarnajayanti Fellowship.

## Notes and references

- R. Guillard, J.-M. Barbe, C. Stern and K. M. Kadish, *The Porphyrin Handbook*, Academic Press, Amsterdam, 2003, pp. 303–349.
- (a) V. Lin, S. DiMaggio and M. Therien, *Science*, 1994, **264**, 1105–1111; (b) A. Tsuda and A. Osuka, *Science*, 2001, **293**, 79–82; (c) S. Ooi, T. Tanaka, K. H. Park, S. Lee, D. Kim and A. Osuka, *Angew. Chem., Int. Ed.*, 2015, **54**, 3107–3111; (d) J. Sankar, H. Rath, V. Prabhuraja, S. Gokulnath, T. K. Chandrashekar, C. S. Purohit and S. Verma, *Chem. – Eur. J.*, 2007, **13**, 105–114.
- T. V. Duncan, K. Susumu, L. E. Sinks and M. J. Therien, *J. Am. Chem. Soc.*, 2006, **128**, 9000–9001.
- (a) F. C. Grozema, C. Houarner-Rassin, P. Prins, L. D. A. Siebbeles and H. L. Anderson, *J. Am. Chem. Soc.*, 2007, **129**, 13370–13371; (b) K. Susumu, P. R. Frail, P. J. Angiolillo and M. J. Therien, *J. Am. Chem. Soc.*, 2006, **128**, 8380–8381; (c) J. Rawson, P. J. Angiolillo and M. J. Therien, *Proc. Natl. Acad. Sci. U. S. A.*, 2015, **112**, 13779–13783.
- (a) Y. Nakamura, S. Y. Jang, T. Tanaka, N. Aratani, J. M. Lim, K. S. Kim, D. Kim and A. Osuka, *Chem. – Eur. J.*, 2008, **14**, 8279–8289; (b) M. Pawlicki, H. A. Collins, R. G. Denning and H. L. Anderson, *Angew. Chem., Int. Ed.*, 2009, **48**, 3244–3266.
- (a) Z. Li, T.-H. Park, J. Rawson, M. J. Therien and E. Borguet, *Nano Lett.*, 2012, **12**, 2722–2727; (b) G. Sedghi, V. M. Garcia-Suarez, L. J. Esdaile, H. L. Anderson, C. J. Lambert, S. Martin, D. Bethell, S. J. Higgins, M. Elliott, N. Bennett, J. E. Macdonald and R. J. Nichols, *Nat. Nanotechnol.*, 2011, **6**, 517–523.
- B. K. Reddy, A. Basavarajappa, M. D. Ambhore and V. G. Anand, *Chem. Rev.*, 2017, **117**, 3420–3443.
- B. K. Reddy, S. C. Gaddekar and V. G. Anand, *Chem. Commun.*, 2016, **52**, 3007–3009.
- S. P. Panchal, S. C. Gaddekar and V. G. Anand, *Angew. Chem., Int. Ed.*, 2016, **55**, 7797–7800.
- T. Y. Gopalakrishna, J. S. Reddy and V. G. Anand, *Angew. Chem., Int. Ed.*, 2014, **53**, 10984–10987.
- K. Goto, T. Kubo, K. Yamamoto, K. Nakasuji, K. Sato, D. Shiomi, T. Takui, M. Kubota, T. Kobayashi, K. Yakusi and J. Ouyang, *J. Am. Chem. Soc.*, 1999, **121**, 1619–1620.
- (a) S. Suzuki, Y. Morita, K. Fukui, K. Sato, D. Shiomi, T. Takui and K. Nakasuji, *J. Am. Chem. Soc.*, 2006, **128**, 2530–2531; (b) K. Uchida, S. Ito, M. Nakano, M. Abe and T. Kubo, *J. Am. Chem. Soc.*, 2016, **138**, 2399–2410; (c) Z. Mou, K. Uchida, T. Kubo and M. Kertesz, *J. Am. Chem. Soc.*, 2014, **136**, 18009–18022.
- E. Fischer, J. Larsen, J. B. Christensen, M. Fourmigué, H. G. Madsen and N. Harrit, *J. Org. Chem.*, 1996, **61**, 6997–7005.
- J. L. Sessler, D.-G. Cho, M. Stępień, V. Lynch, J. Waluk, Z. S. Yoon and D. Kim, *J. Am. Chem. Soc.*, 2006, **128**, 12640–12641.
- Z. Chen, C. S. Wannere, C. Corminboeuf, R. Puchta and P. v. R. Schleyer, *Chem. Rev.*, 2005, **105**, 3842–3888.
- M. Gouterman, *J. Mol. Spectrosc.*, 1961, **6**, 138–163.
- P. J. Angiolillo, J. Rawson, P. R. Frail and M. J. Therien, *Chem. Commun.*, 2013, **49**, 9722–9724.
- M. Kasha, H. R. Rawls and M. Ashraf El-Bayoumi, *Pure Appl. Chem.*, 1965, **11**, 371.
- N. F. Phelan and M. Orchin, *J. Chem. Educ.*, 1968, **45**, 633.
- (a) J. Lykkebo, A. Gagliardi, A. Pecchia and G. C. Solomon, *ACS Nano*, 2013, **7**, 9183–9194; (b) G. C. Solomon, D. Q. Andrews, R. P. Van Duyne and M. A. Ratner, *J. Am. Chem. Soc.*, 2008, **130**, 7788–7789.
- (a) E. Maggio, G. C. Solomon and A. Troisi, *ACS Nano*, 2014, **8**, 409–418; (b) A. B. Ricks, G. C. Solomon, M. T. Colvin, A. M. Scott, K. Chen, M. A. Ratner and M. R. Wasielewski, *J. Am. Chem. Soc.*, 2010, **132**, 15427–15434.
- (a) A. Bandyopadhyay, B. Varghese, H. Hopf and S. Sankararaman, *Chem. – Eur. J.*, 2007, **13**, 3813–3821; (b) M. Gholami and R. R. Tykwinski, *Chem. Rev.*, 2006, **106**, 4997–5027.

